Electronic Supplementary Material (ESI) for Nanoscale.

Supporting information to: "Photonic crystal cavity-enhanced emission from silicon vacancy centers in polycrystalline diamond achieved without postfabrication fine-tuning"

L. Ondič,[1] M. Varga,[1] J. Fait,[1] K. Hruška,[1] V. Jurka,[1] A. Kromka,[1] J. Maňák,[1] P. Kapusta,[2] J. Nováková[3]

[1]Institute of Physics, Czech Academy of Sciences, v.v.i., Cukrovarnická 10, CZ-162 00, Prague 6, Czech Republic; [2]J. Heyrovský Institute of Physical Chemistry, Czech Academy of Sciences, v.v.i., Dolejškova 3, CZ-182 23, Prague 8, Czech Republic; [3]Charles University in Prague, Faculty of Mathematics and Physics, Department of Surface and Plasma Science, V Holešovičkách 742/2, 180 00 Prague 8,

1. Fabrication process

Figure S1 sketches the steps of the fabrication process of the photonic crystal cavities, which is in detail described in the Methods section of the main text.

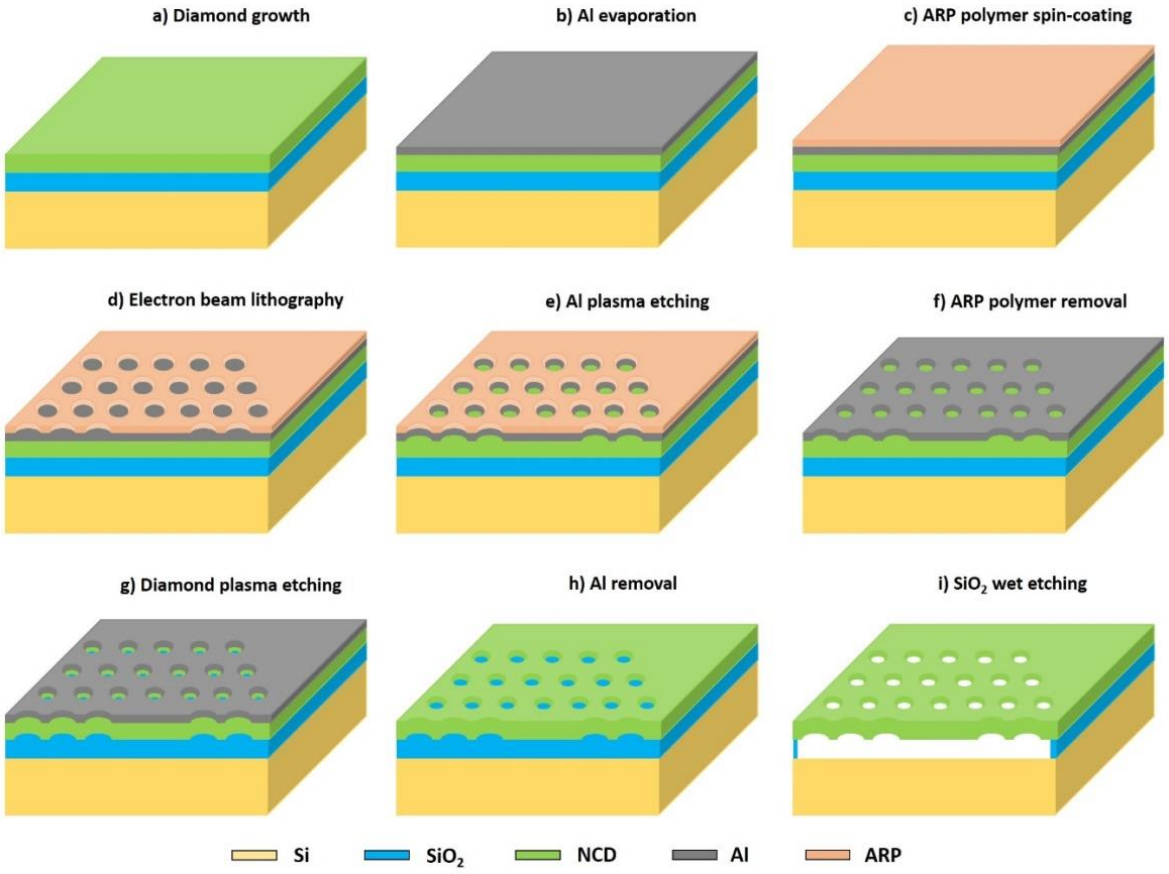

Figure S1: The process flow to fabricate suspended photonic crystal structure with cavity in polycrystalline diamond layer.

2. SEM image of the photonic crystal cavity

During the fabrication process, a photonic crystal (PhC) cavity composed of one missing hole was unintentionally created in the right part of the photonic crystal (Fig. S2). In Fig. 2a of the main text, this cavity is also visible in the micro-photoluminescence spectra.

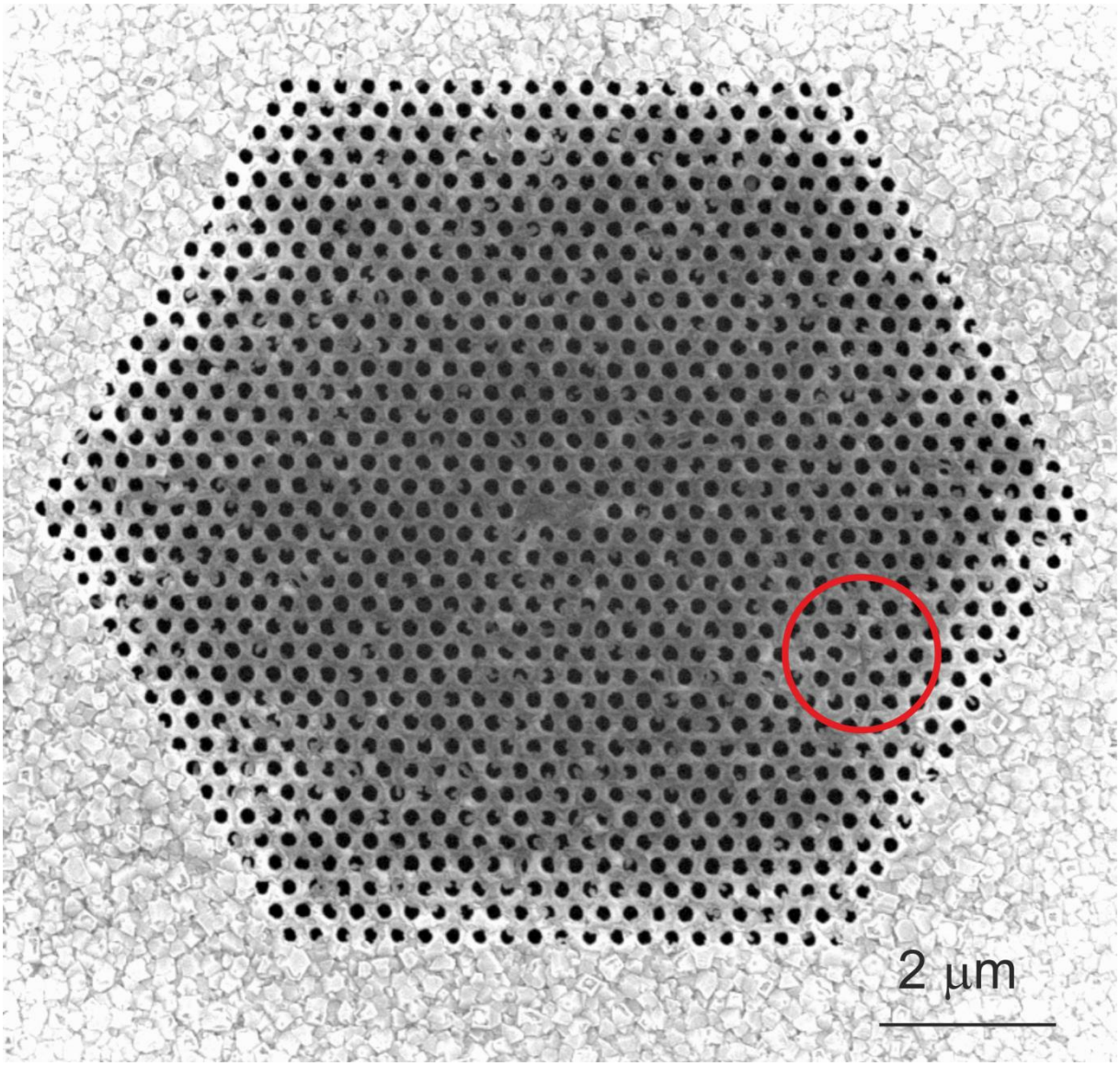

Figure S2: SEM image of the photonic structure discussed in detail in the main text. Encircled is a PhC cavity comprised of a single missing hole.

3. Polarization resolved photoluminescence:

In order to verify the symmetry of the cavity modes, the micro-photoluminescence measurements were realized with a polarization filter in front of the detector. Fig. S3 shows the results obtained on a photonic crystal cavity having the cavity modes red-shifted with respect to the SiV center zero-phonon emission line (cavity No. 1, third row in Fig. 3b of the main text). The obtained results manifest that the e1, e2 (o1, o2) modes have in the far-field most of the electrical field perpendicular (parallel) with respect to the cavity orientation. This is in accordance with the results of the simulations of the electric fields of the modes shown in Fig. 2c of the main text. Namely, the *Ex* component of the e1 mode will cancel itself in the far-field due to its anti-symmetric nature along both the *x* and *y*-direction, whereas the *Ey* component is symmetric. For the o1, the opposite is true, thus the *Ex* component (oriented along the cavity) of the electric field is dominant in the far-field.

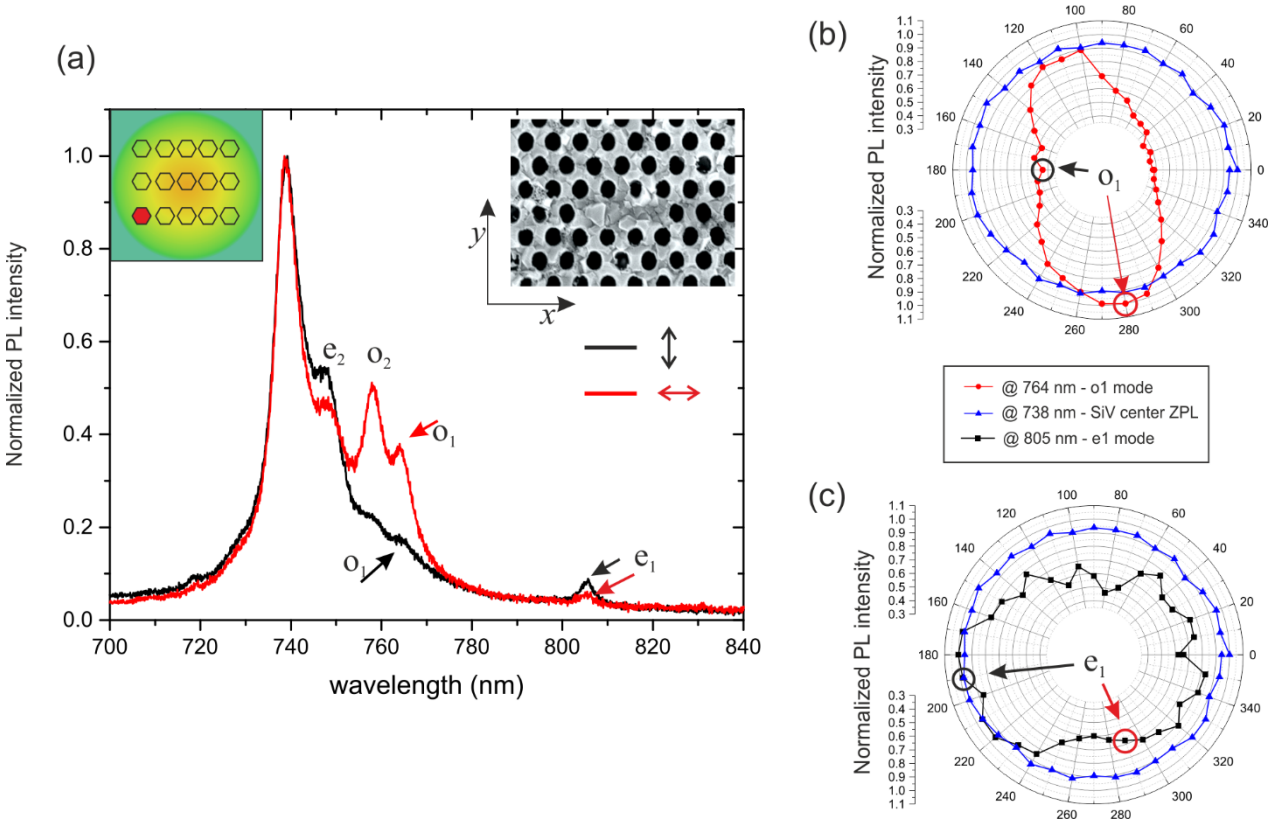

Figure S3: Polarization-resolved micro-photoluminescence measurements on a photonic crystal cavity (cavity No.1 in the third row of cavities within the fabricated sample).

4. Computation of collection efficiency

In order to obtain a relevant comparison between the measured photoluminescence intensity of the (i) PhC cavity, (ii) the reference (a photonic crystal slab surrounding the cavity) and (iii) the "smooth" pristine diamond layer, we have computed a collection efficiency of the employed optics (objective with NA 0.9).

Employing a finite-difference time-domain (FDTD) method implemented in the free software MEEP, we have simulated a propagation of the electromagnetic flux from a point pulsed source placed in a planar diamond layer, in a photonic crystal and in a photonic crystal cavity with relevant dimensions. We have used a 3D computation cell in the middle of which the investigated structure was placed. The thickness of the layers used in the simulations is 200 nm whereas the final sample had thickness slightly lower (around 185 nm). The simulations were done before the sample was fabricated and it would be time-consuming to repeat all of them for the thickness of 185 nm and it would not bring qualitatively different results. We have verified (for few cases) that also quantitatively, the results differ negligibly compared to the uncertainty given by the structural imperfections (roughness etc.). The only difference is in spectral position of the modes. Fig. S4a shows a schematic sketch of the cross-section of the computational cell with a diamond slab (planar diamond layer). The total extraction efficiency in the upwards direction (the collection efficiency by our objective with NA=0.9) was computed by dividing the total flux propagating upwards (the flux within the collection cone given by the NA=0.9) with the total flux emitted by the source.

The SiV centers have no preferential orientation in the diamond layer due to the random orientation of the diamond grains, which form the layer. Therefore, their emission can be in the simulation approximated by the dipoles with Ex, Ey and Ez orientations having the same contribution to the overall emission intensity. However, we would like to stress that their contribution to the total intensity detected via the objective with NA=0.9 is not the same. Namely, we have theoretically verified (not shown) that the contribution of the *Ez* component is at least of factor 10 lower in comparison to the *Ex* and *Ey* within the spectral region of interest and can be therefore neglected in the analysis.

First, let us compare results obtained for the smooth diamond slab and the diamond photonic crystal slab. The results are summarized in Fig. S4. The lateral position of the source within the hexagonal lattice of the PhC is depicted in the inset of Fig. S4c. The total extraction efficiency in the upwards direction from the diamond slab is below 7% in the investigated spectral region due to total internal reflection on the diamond-air interface (Fig. S4b). Towards the objective with NA=0.9, only less than 4% of the total flux propagates. For the PhC, the upwards extraction efficiency is 0.5 (50%) in the region of the photonic band gap. The objective collects up 40% of the emitted light within the bandgap. Due to the hexagonal symmetry, the results slightly differ for the distinct in-plane light polarizations, *Ex* and *Ey*.

The Purcell factor of the emitter within the PhC is defined by the amount of total flux emitted by the source within the photonic crystal slab divided by the total flux emitted by the same source inside the homogenous bulk diamond. Due to decreased (modified) local density of states within the bandgap (out of the bandgap) of the photonic crystal, the Purcell factor is lower than (differs from) the unity (Fig. S4c). For the simulated case of the source placed in the middle of the hexagonal

lattice, the Purcell factor is below 0.05 for the *Ex* polarization and below 0.25 for the *Ey* polarization for the wavelengths within the photonic bandgap. The value of the Purcell factor reflects into the final performance of the PhC slab given by the value of the emission enhancement factor, which we define as a ratio of the total upwards extracted flux from the PhC slab to that of the planar slab. Figure S4e plots the emission enhancement factor for both the *Ex* and *Ey* polarizations of the source and it is clear that for the *Ex* polarization, the flux that we extract from the PhC slab is lower than that from the planar slab (ratio of the fluxes being lower than unity). On the other hand, for the *Ey* polarization, the situation is opposite (the ratio being higher than unity). In summary, even though the extraction efficiency enhancement of the PhC (ratio of the extraction efficiency from the PhC slab to that of the planar layer) is high for both source polarizations (Fig. S4d) due to the existence of the photonic bandgap, the extracted energy enhancement factor strongly depends on the polarization of the source due to the Purcell effect. Furthermore, this factor depends also on the position of the source within the photonic crystal lattice as shown in Fig. S5, where the results of simulations for 4 positions of always two point sources (one with *Ex* and the other with *Ey* polarization) are plotted.

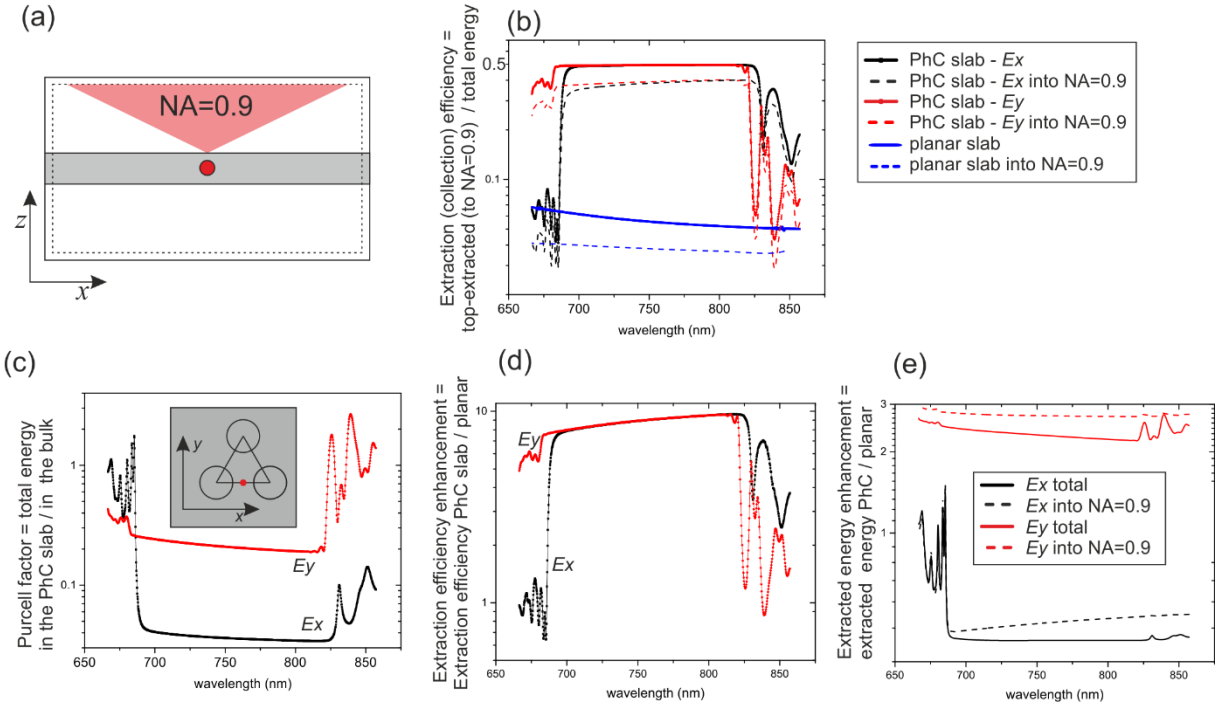

Figure S4: (a) Cross-section of the 3D FDTD computational cell. Point source (red dot) is positioned in the middle of the cell inside of a thin diamond planar slab. The solid rectangle depicts the borders of the cell. The dashed-line rectangle depicts the detectors used for computing the flux from the source. The red color-filled triangle depicts the collection area of the employed objective. (b) Computed extraction (collection) efficiency into upper direction (into the NA=0.9 given by the objective used in experiments) from a point source in a planar diamond slab and a photonic crystal diamond slab. For details see the text. (c) Purcell enhancement factor for source positioned (vertically) in the middle of the photonic crystal slab. Both in-plane perpendicular polarizations of the source are considered. Inset shows the lateral position within the lattice. (d) Extraction efficiency enhancement provided by the photonic crystal slab with respect to the planar slab. (e) Factor showing the enhancement of the extracted flux from the photonic crystal slab with respect to the planar slab.

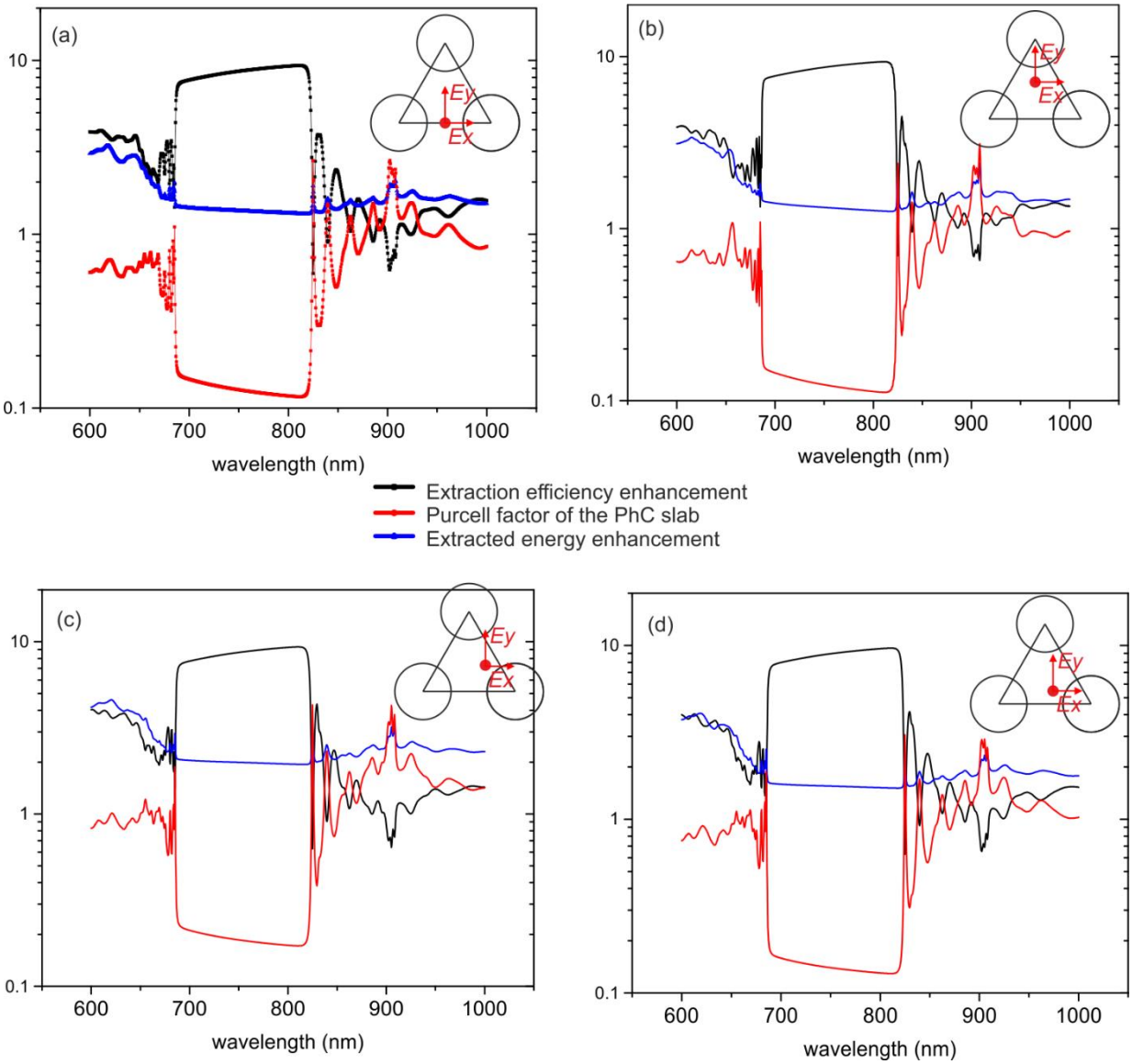

Figure S5: Results of the FDTD simulation for always two point sources having perpendicular in-plane polarizations, *Ex* and *Ey,* positioned at the same position. (a-d) Sources inside the diamond PhC slab at various lateral positions with respect to the hexagonal lattice. The sources are depicted by the red dots in the insets. In the vertical direction, the source is placed in the middle of the slab.

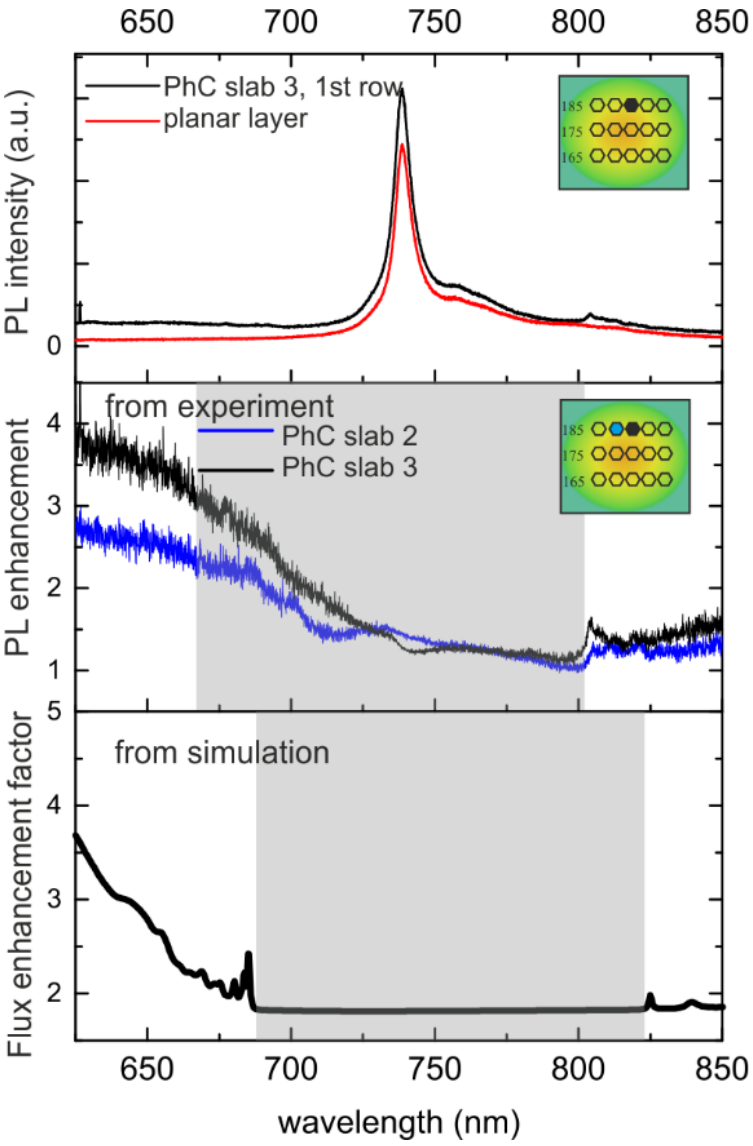

Figure S6: Top: Measured (objective with NA=0.9) PL intensity from the PhC slab surrounding the PhC cavity (the one which enabled 2.4 enhancement of SiV centers emission) and from the planar slab (detached from the substrate) around it. Middle: PL enhancement factor of the PhC slab No. 2 and 3, 1st row of cavities. The gray-shaded area depicts the photonic band gap. Bottom: Simulated flux enhancement factor in the collection cone of NA=0.9 for the PhC slab.

Figure S6 compares the experimentally acquired PL enhancement factor with the theoretical curve obtained by averaging the results for the 4 positions of the *ExEy* source in the PhC slab. We have theoretically verified (not shown) that the contribution of the *Ez* component can be neglected in comparison to the *Ex* and *Ey* in the analysis. The experimental curve qualitatively very well resembles the simulated one taken into account that the simulation does not include losses of the system or structural imperfections. Also, in the real sample, the emitters are distributed homogeneously within the whole thickness of the slab whereas the simulations account only for emitters vertically in the middle of the slab. Therefore, in order to get more precise results, simulations should be performed for more positions of the sources. This is, however, out of scope of this paper. In the long-wavelength part, the photonic band edge states manifested by peaks at the edge of the photonic band gap can be clearly recognized in both the experimental and theoretical results. The band gap of the real structure is blue-shifted with respect to the simulated one due to slightly lower thickness (185 nm in the sample vs 200 nm in the simulation). The experimental PL enhancement factor, which spans from 1.1 to 1.5 above 725 nm is slightly lower than the simulated one being above 1.8 due the reasons listed above.

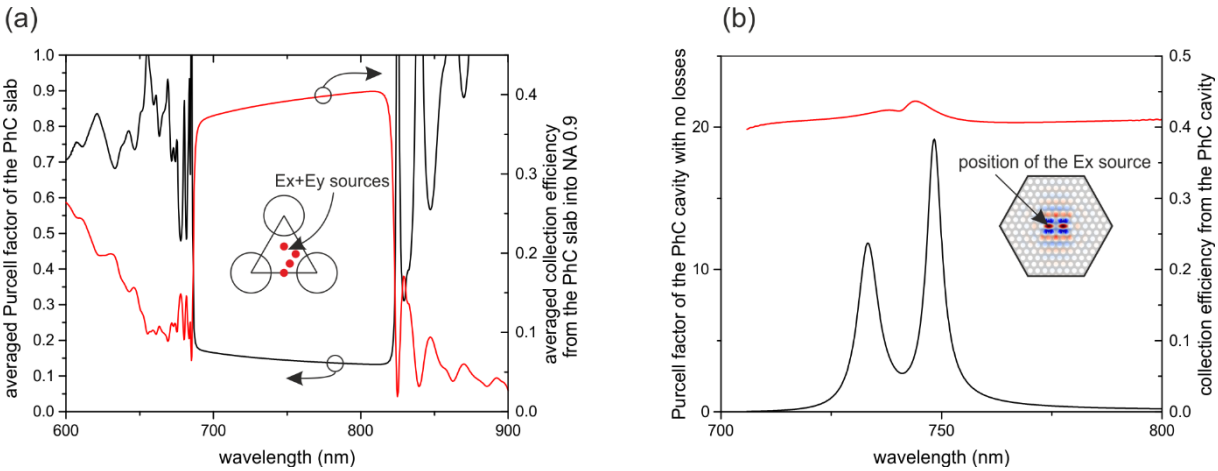

Figure S7: (a) Computed Purcell factor of the diamond PhC slab in comparison with computed collection efficiency of the objective having NA 0.9, averaged over 4 positions (see the Inset) of the source having both in-plane components of the electric field (*Ex* and *Ey*). (b) Purcell factor and the collection efficiency from the L3 PhC diamond cavity with the source having only *Ex* component and placed in the ideal position for coupling into the o1 mode (see the Inset), the mode spectrally overlapping the zero-phonon line of the SiV centers. Note that the modes in the simulation are slightly red-shifted with respect to the experiment because a slightly thicker diamond was employed in the simulation. Furthermore, the simulation is done for ideal diamond with no losses, thus the Purcell factor is approx. twice higher than that considered in the main text.

Figure S7 shows results of the simulations that were used for evaluating the collection efficiencies and the Purcell factor from the PhC slab and the PhC cavity, respectively. For the case of the PhC slab, the curve is an average over the 4 positions of the source already discussed in Fig. S5. The source has both in-plane components of the electric field because the Purcell enhancement strongly depends also on the polarization. For the case of the PhC cavity, we have chosen to take into account only the ideal case of the emitter position and polarization with respect to the coupling into the o1 mode – the mode in spectral overlap with the zero-phonon line of the SiV centers. This approach gives us the maximal possible Purcell enhancement that could be achieved in the ideal case of the emitter polarization and position. Furthermore, for the sake of simplicity, the optical losses were not included in the simulation and therefore, the computed Purcell factor is higher than that used in the main text.

5. Purcell factor analysis

In a 200 nm thin homogeneous diamond layer, the FDTD simulation yields the collection efficiency η_{hom} = 0.039 with the NA=0.9 objective at the wavelength of the o1 mode (Fig. S4b). The collection efficiency is low due to total internal reflection on diamond air interface and due to the fact that the emission is guided within the layer. The theoretical Purcell factor of the emitter in the middle of the 200 nm thin diamond layer F_{hom}=0.8. It was computed as a ratio of the total emission intensity from the emitter in the 200 nm thin diamond layer and the emission intensity of the emitter inside a bulk diamond employing the FDTD simulation.

In the PhC cavity, the η_{cav} = 0.42 and the theoretical Purcell factor F_{cav} equals to 13 for a single emitter inside the maximum of the local density of optical states of the mode o1 as estimated in the main text.

In the PhC structure which surrounds the PhC cavity, the η_{PhC} = 0.39 and the averaged theoretical F_{PhC}=0.15 at the wavelength of the o1 mode (Fig. S7a).

From the above numbers, the expected photoluminescence intensity ratio of the structures at the wavelength of the o1 mode, which spectrally overlaps the SiV centers emission, can be evaluated.

For the ratio of PL intensity from the PhC and the homogeneous thin layer, we get (at the wavelength of the o1 mode)

$$\frac{I_{PhC}}{I_{hom}} = \frac{\eta_{PhC}\, F_{PhC}}{\eta_{hom} F_{hom}} = 1.875.$$

This ratio is already plotted and discussed in Figure S6. In comparison with the experimental value of 1.3 of the PL intensity enhancement, the theoretical value is slightly higher. Using the experimental value of the PL intensity enhancement, the Purcell factor of the fabricated PhC structure can be evaluated while keeping the $\eta_{hom}, F_{hom}, \eta_{PhC}$ from the simulation. The experimental PhC Purcell factor is $F_{PhC}^{experiment} \sim 0.104$. It slightly differs from the theoretical value because it includes imperfections of the real structure (scattering and absorption) and also averages over all the emitter positions (in the simulation, only 4 positions were included, furthermore, the emitters were positioned vertically in the middle of the layer).

Now, we want to compare the performance of the PhC cavity with the 200 nm thin homogeneous diamond layer and the PhC structure, respectively.

For the ratio of PL intensity from the PhC cavity and the homogeneous thin layer, we get

$$\frac{I_{cav}}{I_{hom}} = \frac{\eta_{cav}\, F_{cav}}{\eta_{hom} F_{hom}} = 175$$

For the ratio of PL intensity from the PhC cavity and the PhC crystal, we get

$$\frac{I_{cav}}{I_{PhC}} = \frac{\eta_{cav}\, F_{cav}}{\eta_{PhC} F_{PhC}} = 93.$$

However, the above numbers are expected when a single emitter is positioned in the maximum of the cavity mode. For the ensemble of emitters, the situation is different as discussed below.

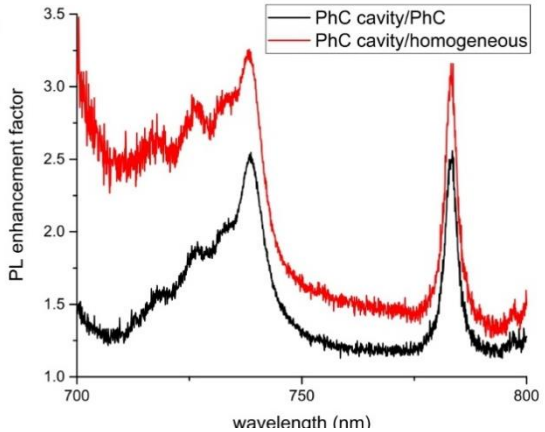

Figure S8: PL intensity ratio of the PhC cavity and PhC structure (black) compared to the PL intensity ratio of the PhC cavity and the homogenous diamond slab (red).

From the experiment we know that the enhancement factor of PL intensity of the PhC cavity to the PL intensity of homogeneous diamond layer equals to approximately 3.2 at the zero-phonon line of the SiV centers (Fig. S8). Using this value, an ensemble-averaged Purcell factor of the fabricated PhC cavity $F_{cav}^{ensemble}$ can be extracted, while taking the other parameters from the simulation. It yields

$$3.2 = \frac{I_{cav}}{I_{hom}} = \frac{\eta_{cav}\, F_{cav}}{\eta_{hom} F_{hom}} = \frac{0.42 * F_{cav}^{ensemble}}{0.039 * 0.8}$$

Then $F_{cav}^{ensemble} = 0.23$.

Also, the ratio of PL intensity from the PhC cavity and from the PhC is known from the experiment. It equals to 2.5 at the zero-phonon-line of the SiV centers (Fig. S8). Again, the ensemble-averaged Purcell factor of the cavity can be extracted, while taking the collection efficiencies from the simulation and the experimental Purcell factor of the PhC $F_{PhC}^{experiment}$. It yields

$$2.5 = \frac{I_{cav}}{I_{PhC}} = \frac{\eta_{cav}\, F_{cav}}{\eta_{PhC} F_{PhC}^{experiment}} = \frac{0.42 * F_{cav}^{ensemble}}{0.39 * 0.104}$$

Then $F_{cav}^{ensemble} = 0.24$. The agreement with the value obtained from the comparison with the homogenous layer is perfect.

Clearly, the experimentally-obtained ensemble-averaged cavity Purcell factor is much lower than the theoretical Purcell factor of a single emitter in the ideal position within the PhC cavity. It is also lower than the Purcell factor of the emitters within the homogeneous layer. The reason is very simple and logical. While exciting the PhC cavity via the objective, the excitation spot is at least 600 nm in diameter and it penetrates through the whole 200 nm thin membrane. This means that all SiV centers within the excitation volume are excited and the emitted light is collected by the objective. Within the excitation volume, three types of emitters are present (i) centers that emit preferentially into Ex and Ey polarization and in the same time are positioned such that they overlap with the cavity mode, (ii) centers that emit preferentially into Ex and Ey polarization and in the same time are positioned such that they do not overlap with the cavity mode, and (iii) centers that emit preferentially into vertical polarization Ez. For the emitters of type (i), the Purcell factor is expected

to be larger than unity but it should be stressed that only a few percent of emitters will be close to the above-mentioned theoretical value of 13. For the emitters of type (ii), the Purcell factor is lower than unity and it is comparable to the Purcell factor of the PhC, and for the emitters of type (iii), the Purcell factor is comparable to that of the homogenous layer. This altogether leads to the experimentally obtained value of the Purcell factor. The evaluation of the exact contribution of each of the type of emitters to the final value is beyond the scope of this paper. However, the following conclusion can be made.

The fact that the $F_{cav}^{ensemble} > F_{PhC}^{experiment}$ proves that light from emitters overlapping the cavity modes couples to these modes and hence enhances the emission rate. This is also clear by the fact that the cavity modes are visible in the PL spectra. The Purcell factor being lower than unity for the cavity modes is due to the fact the measurements are done on the ensemble of emitters. The similar effect was measured also by other groups using the ensemble of SiV centers coupled to cavities [1,2]. If only a single emitter was present within the cavity or if a single emitter from the ensemble could be excited, the values of the experimental factor should be close to the theoretical one.

6. The decay rate

The decay rate was measured on the PhC cavity, on the surrounding PhC and also on the homogenous diamond membrane. The decay rates are within the detection error similar (see inset of Fig. 2 in the main manuscript). This may seem to be in contradiction with the above discussed Purcell factors. However, it has to be stressed that the Purcell factor affects only the radiative rate of the system[3] but the measurement contains the total decay rate including the non-radiative rate. Therefore, when the system decays in a large extent via non-radiative channels, the effect of the Purcell factor on the total decay rate may remain below the resolution of the detector.

The measured decay rate τ at zero-phonon-line is composed of radiative decay rate $\tau_r$and non-radiative decay rate τ_{nr}into phonon wing and into other non-radiative channels. It is defined by a formula

$$\frac{1}{\tau} = \frac{1}{\tau_r} + \frac{1}{\tau_{nr}}$$

If emission into free space is neglected, the Purcell effect affects only the radiative decay rate such that ${\tau_r}^{hom} = \tau_r/F_{hom}$; ${\tau_r}^{PhC} = \tau_r/F_{PhC}$; ${\tau_r}^{cav} = \tau_r/F_{cav}$ where τ_r is a decay rate of the SiV centers in the bulk diamond.[3]

Let`s compare total decay rates of the PhC and the homogenous diamond layer because for those two structures the Purcell factors differ the most. For the PhC crystal it holds that ${1}/{\tau^{PhC}} = {1}/{\tau_r^{PhC}} + {1}/{\tau_{nr}^{PhC}}$ and for the homogenous layer it is ${1}/{\tau^{hom}} = {1}/{\tau_r^{hom}} + {1}/{\tau_{nr}^{hom}}$. We are interested in the ratio of τ^{PhC} and τ^{hom}. If we consider the non-radiative decay rate of the emitters within the PhC being similar to that of the emitter inside the thin layer, we get

$$\frac{\tau^{PhC}}{\tau^{hom}} = \frac{\frac{\tau_r^{PhC} * \tau_{nr}^{PhC}}{\tau_r^{PhC} + \tau_{nr}^{PhC}}}{\frac{\tau_r^{hom} * \tau_{nr}^{hom}}{\tau_r^{hom} + \tau_{nr}^{hom}}} = \frac{\tau_r/F_{PhC} * \tau_{nr}}{\tau_r/F_{PhC} + \tau_{nr}} = \frac{\frac{1}{F_{PhC}}(\tau_r/F_{hom} + \tau_{nr})}{\frac{1}{F_{hom}}(\tau_r/F_{PhC} + \tau_{nr})} = \frac{\tau_r + F_{hom}\,\tau_{nr}}{\tau_r + F_{PhC}\,\tau_{nr}}$$

This is a reasonable approximation based on the fact that we are not changing intrinsic properties of the material. The fact that we may be introducing some surface defects during the PhC fabrication can be neglected.

Now, the quantum yield ϕ of the ensemble of SiV centers is not known for our sample, however, we will consider the value that can be found in literature, which is approximately ϕ=0.05.[4] The quantum yield relates to the decay rate in the following way : $\phi = {}^{\tau}/_{\tau_r}$.[5] When the relevant formula for the τ and the value of the 0.05 is inserted, we get $\tau_r = 19\,\tau_{nr}$. Now, we can input this value to the above formula and get:

$$\frac{\tau^{PhC}}{\tau^{hom}} = \frac{\tau_r + F_{hom}\,\tau_{nr}}{\tau_r + F_{PhC}^{experiment}\tau_{nr}} = \frac{19\,\tau_{nr} + 0.8\,\tau_{nr}}{19\,\tau_{nr} + 0.104\,\tau_{nr}} = 1.036$$

This means that with the given properties of the system, we can expect only a 3.6% change (prolongation) of the decay measured on the PhC with respect to the decay on the homogeneous layer. For the case of the PhC and the PhC cavity, after substituting experimental values for the Purcell factors, the ratio of ${}^{\tau^{cav}}/_{\tau^{PhC}} \sim 0.993$. Both these values are below the resolution of our detection system, which explains the similar measured decay for all the studied structures.

7. Modes localized in random structural defects

Here we show by FDTD simulation that unintentional structural defects in the photonic crystal slab lattice also support photonic modes. An example is given in Fig. S9 where the defects from the real photonic structure (PhC cavity No.2, first row, see also Fig. 3 in the main text) were taken into account in simulation. A defect, which consists of a hole with significantly reduced diameter, is localized close to the main L3 PhC cavity. Consequently, the emission of the source at specific wavelength placed in the main PhC cavity can couple to this adjacent defect, which can be clearly seen on Fig. S9. This leads to the appearance of additional photonic modes in the cavity spectrum. Indeed, we observed more than five cavity modes in some cases, which is most probably caused by the presence of such defects. Note that the precise simulation of the structures is not possible from the SEM images, because they do not offer the complete 3D information about the structure.

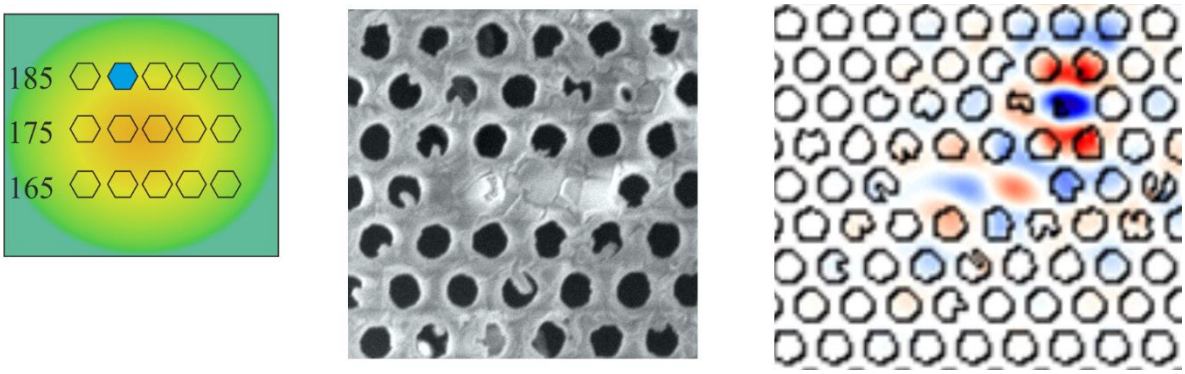

Figure S9: Left: Position of the investigated structure within the sample – PhC cavity No. 2, 1st row. Middle: SEM image of the cavity. Right: Electric field (component along with the cavity) profile of the mode coupled to the unintentionally created structural defect in close proximity of the cavity.

References:

(1) Fehler, K. G.; Ovvyan, A. P.; Antoniuk, L.; Lettner, N.; Gruhler, N.; Davydov, V. A.; Agafonov, V. N.; Pernice, W. H. P.; Kubanek, A. Purcell-Enhanced Emission from Individual SiV- Center in Nanodiamonds Coupled to a Si3N4-Based, Photonic Crystal Cavity. *arXiv:1910.06114 [cond-mat, physics:quant-ph]* **2019**.

(2) Riedrich-Möller, J.; Kipfstuhl, L.; Hepp, C.; Neu, E.; Pauly, C.; Mücklich, F.; Baur, A.; Wandt, M.; Wolff, S.; Fischer, M.; Gsell, S.; Schreck, M.; Becher, C. One- and Two-Dimensional Photonic Crystal Microcavities in Single Crystal Diamond. *Nature Nanotechnology* **2012**, *7* (1), 69–74. https://doi.org/10.1038/nnano.2011.190.

(3) Pelton, M. Modified Spontaneous Emission in Nanophotonic Structures. *Nature Photon* **2015**, *9* (7), 427–435. https://doi.org/10.1038/nphoton.2015.103.

(4) Turukhin, A. V.; Liu, C.-H.; Gorokhovsky, A. A.; Alfano, R. R.; Phillips, W. Picosecond Photoluminescence Decay of Si-Doped Chemical-Vapor-Deposited Diamond Films. *Phys. Rev. B* **1996**, *54* (23), 16448–16451. https://doi.org/10.1103/PhysRevB.54.16448.

(5) Pelant, I.; Valenta, J. *Luminescence Spectroscopy of Semiconductors*; Oxford University Press.